

## Quasi-Periodic Releases of Streamer Blobs and Velocity Variability of the Slow Solar Wind near the Sun

H.Q. Song<sup>1,2</sup> · Y. Chen<sup>1</sup> · K. Liu<sup>3</sup> ·  
S.W. Feng<sup>1</sup> · L.D. Xia<sup>1</sup>

Received: ●●●●●●●● / Accepted: ●●●●●●●● / Published online: ●●●●●●●●

**Abstract** We search for persistent and quasi-periodic release events of streamer blobs during 2007 with the Large Angle Spectrometric Coronagraph on the *Solar and Heliospheric Observatory* and assess the velocity of the slow solar wind along the plasma sheet above the corresponding streamer by measuring the dynamic parameters of blobs. We find 10 quasi-periodic release events of streamer blobs lasting for three to four days. In each day of these events, we observe three-five blobs. The results are in line with previous studies using data observed near the last solar minimum. Using the measured blob velocity as a proxy for that of the mean flow, we suggest that the velocity of the background slow solar wind near the Sun can vary significantly within a few hours. This provides an observational manifestation of the large velocity variability of the slow solar wind near the Sun.

**Keywords:** Corona, Solar wind, Velocity Fields

### 1. Introduction

Sheeley *et al.* (1997) were the first to report the observation of plasma blobs, released from the tips of streamers as revealed in the data obtained by the Large Angle Spectrometric Coronagraph (LASCO) on the *Solar and Heliospheric Observatory* (SOHO) spacecraft (Brueckner *et al.*, 1995) around the last solar minimum. According to the data analysis by Sheeley *et al.* (1997) and a series of following studies by Wang *et al.* (1998,2000) blobs emerge at about 2-4 Solar Radii ( $R_{\odot}$ ) from the Sun center as radially elongated structures with initial sizes being about 1  $R_{\odot}$  in the radial direction and 0.1  $R_{\odot}$  in the transverse direction. They move outward radially, maintaining an almost constant angular

---

<sup>1</sup> School of Space Science and Physics, Shandong University at Weihai, Weihai Shandong 264209, China  
email: yaochen@sdu.edu.cn

<sup>2</sup> State Key Laboratory of Space Weather, Chinese Academy of Sciences, Beijing 100190, China

<sup>3</sup> School of Earth and Space Sciences, University of Science and Technology of China, Hefei Anhui 230026, China

span and their lengths increased from  $\approx 1 R_{\odot}$  to  $\approx 3 R_{\odot}$  within the LASCO field of view (FOV). Their velocities also increase gradually with increasing length. Besides understanding the plasma process accounting for the formation of blobs themselves, there are at least two other issues directly related to blob studies: The first is that blob studies provide a practical technique of assessing the velocity of the embedded solar wind, since blobs are believed to get closely coupled to and flow outward together with the background solar wind shortly after their emission. This component of the solar wind (*i.e.*, the wind originated from the plasma sheet above a streamer) is usually taken to be a part of the slow solar wind (*e.g.*, Woo and Martin, 1997; Sheeley *et al.*, 1997; Habbal *et al.*, 1997; Wang *et al.*, 2000). That is to say that the measurements of the blob motion can be used to represent the velocity of the embedded slow wind plasmas above a certain distance. Another issue of blob studies concerns the possible diagnostics of plasma properties enclosed in the closed magnetic-field regions of streamers, especially, in the streamer cusp region, through *in situ* detection of blob structures in interplanetary space. This is deduced from the assumption that blobs originate from inside the closed arcades right below the streamer cusp, which is used or supported by several physical and numerical models of blob formation (*e.g.*, Wu *et al.*, 2000; Wang *et al.*, 2000; Chen *et al.*, 2009). Note that there are also models that suggest that blobs are the aftermath of magnetic reconnections along the current sheet embedding in the solar wind with open magnetic geometry (*e.g.*, Einaudi *et al.*, 1999; Lapenta and Knoll, 2005). The possibility of collecting samples of plasmas originated from inside the closed magnetic-field regions with *in situ* measurements is important for the evaluation of elemental compositions in the blob source region, and for understanding the formation and stability of coronal streamers, as well as the delicate coupling process between plasmas and magnetic field near the cusps.

Wang *et al.* (1998) reported a very interesting event with steady quasi-periodic releases of blobs above a streamer during the eight days from 19 to 26 April, 1997. The daily rate of blobs in this event is observed to be three-five with a release period ranging from five to eight hours. To interpret the formation and quasi-periodic releases of blobs, Chen *et al.* (2009) designed a numerical model accounting for the magnetohydrodynamic coupling process between the closed streamer magnetic arcades and the solar wind expansion. They found that the streamer-cusp geometry is subject to an intrinsic instability originating from the peculiar magnetic topological feature at the cusp region despite the long-term stability of the overall morphology. According to Chen *et al.* (2009), the process of the instability consists of two successive processes. One is the plasma magnetic-field expansion through the localized cusp region where the field is too weak to maintain plasma confinement; the continuing expansion brings strong velocity shear into the slow wind regime, providing the free energy necessary for the onset of a streaming sausage mode instability (Lee, Wang, and Wei, 1988; Wang, Li, and Wei, 1988). The other is then the onset and nonlinear development of the streaming instability, which causes pinches of magnetic-field lines and drives reconnections at the pinching points to form separated magnetic blobs. After the birth of a blob, the streamer system returns to the configuration with a lower cusp point, subject to another cycle of the instability. As mentioned, the

whole process originates from the topological feature at the cusp region, which is intrinsically associated with a typical coronal streamer; therefore Chen *et al.* (2009) made use of the word “intrinsic” to describe the streamer instability. We point out in passing that other numerical models demonstrating various aspects of streamer instabilities exist in the literature (*e.g.*, Suess, Wang, and Wu, 1996; Wu *et al.*, 2000; Endeve, Leer, and Holzer, 2003; Endeve, Holzer, and Leer, 2004). According to the numerical results given by Chen *et al.* (2009), the period of blob formation is about four-five hours. Thus, hypothetically, one can observe four-six blobs per day on average, in agreement with what is observed by Wang *et al.* (1998). We find this agreement with the observations to be very encouraging considering the simplicity of Chen *et al.*’s numerical model (2009). However, in the series of blob studies by Wang *et al.* (1998,2000), only a few events with continuous and quasi-periodic releases of blobs are reported (in April 1997 and December 1998). If the scenario proposed by Chen *et al.* (2009) is basically correct—that the blobs are the aftermath of an intrinsic instability of coronal streamers with release periods being several hours—there should exist more events with steady blob releases. It is the primary purpose of this paper to search for events similar to those reported by Wang *et al.* (1998) with the LASCO data. As a starting point, we only deal with the data accumulated in the whole year of 2007 in this paper.

As mentioned previously, the velocity measurement of blobs can be used as a proxy for that of the embedded slow solar wind along the plasma sheet. This argument is further supported by a recent numerical calculation presented in Chen *et al.* (2009). They show that, as a result of the dynamical coupling to the mean flow, the blobs are basically accelerated to the same velocity after they further propagate a distance of 2-3  $R_{\odot}$  from the disconnection point. Therefore, in general, beyond a certain heliocentric distance of, say, 5 to 7  $R_{\odot}$ , the background solar wind velocity can be well represented by that of the blobs. However, most blobs are too weak to be observable beyond 20  $R_{\odot}$  by the LASCO C3 coronagraph. Therefore, the major region where this method is usable is limited to 4-20  $R_{\odot}$ . At present, there are only a few other indirect techniques, such as the Doppler dimming technique (*e.g.*, Li *et al.*, 1998; Cranmer *et al.*, 1999; Strachan *et al.*, 2002) and the IPS (Interplanetary Scintillation) technique (*e.g.*, Grail *et al.*, 1996; Breen *et al.*, 1999), that can be used to determine the wind velocity within the first 20  $R_{\odot}$  of the corona. For instance, one can use the measured ratio of the O VI doublet to evaluate the outflowing velocities of O<sup>5+</sup> ions. The velocities obtained by both the Doppler dimming technique and the IPS techniques are usually model dependent with large errors. As mentioned, the presence of blobs provides another velocity diagnostic technique of the solar wind in the corona. This can be referred to as the blob technique. Among the various methods of velocity measurement in the corona, the blob technique may serve as the most accurate, at least in cases where blobs are clearly measurable. One serious limitation of this method is that only the projected velocity of the solar wind along the plasma sheet can be revealed. Also, it should be noted that the blob technique is based on the general assumption that blobs can be taken as effective velocity tracers of the mean flow. Nevertheless, the second purpose of this paper is to examine the velocity of the solar wind along the plasma sheet,

which is usually regarded as a part of the source region of the slow solar wind, as mentioned previously. The details of our observations and results are described in the following section. The summary and discussion are provided in the last section of this paper.

## 2. Observations and Results

As already mentioned, one of the main purposes of this paper is to search for steady release events of blobs. To investigate the quasi-periodic character of blob emissions, we need to observe enough blobs emitted above a streamer. Therefore, only those events with emission lasting for at least three days are reported in this study. By examining all of the white-light data taken by the LASCO coronagraph in 2007, we have identified 10 events with steady emission of blobs lasting for three to four days. Some information about these 10 events is listed in Table 1, where the number in the first column indicates the time sequence of the blob emission. In the remaining columns, we list the start and end dates of the events, the position angle (PA) of the central axis of the streamers from which blobs are released, the total number of blobs and the average daily rate released during the event, and the minimum and maximum values of the blob velocities at a specific height, say,  $9 R_{\odot}$ . The PA increases counterclockwise, taken to be zero in the northward direction. The varying ranges of the deduced blob accelerations are also presented in the last column of this table. The velocities and accelerations given in this table are projected quantities on the plane of the sky, which are obtained with a second-order polynomial fitting to the measured blob tracks. The details of our data reduction method will be introduced as we proceed.

**Table 1.** Information on the 10 events with quasi-periodic releases of blobs lasting for three-four days observed in 2007.

No.	Observation date	PA ( $^{\circ}$ )	Total number /avg. daily rate	Velocity range at $9 R_{\odot}$ ( $\text{km s}^{-1}$ )	Acceleration range ( $\text{m s}^{-2}$ )
1	Feb 14-16	103	11/3.7	183-356	3.6-14.2
2	Apr 04-07	248	12/3	191-335	1.1-13.8
3	Apr 25-27	288	9/3	197-299	1.3-6.2
4	Apr 30-May 2	246	9/3	169-298	0.6-8.0
5	May 07-09	71	10/3.3	240-400	3.6-18.2
6	Jun 05-08	67	13/3.3	173-303	2.6-11.4
7	Jun 13-15	119	12/4	228-379	2.2-17.8
8	Jun 30-Jul 2	69	10/3.3	162-287	2.2-11.2
9	Jul 18-20	106	11/3.7	200-334	3.9-10.4
10	Sep 27-29	244	9/3	192-286	2.2-11.0

The blob structures are only marginally brighter than the background coronal emission, as seen from the white-light brightness and polarization measurements by LASCO (Sheeley *et al.*, 1997; Wang *et al.*, 1998). Therefore, it is generally difficult to recognize a blob from the original coronagraph images. The usual

way to emphasize the blob features is to make running-difference images by subtraction of two successive images taken tens of minutes to one hour apart in time. After this procedure, the blob structures are more easily identified. They reveal themselves as radially elongated white-leading-black bipolar islands. The white (black) color indicates a brightness increase (decrease) in the corresponding region during the elapsed interval. In the following discussion, we first introduce our data analysis method by presenting two examples observed during 13 to 15 June and during 30 June to 2 July, which are the seventh and eighth events listed in Table 1 and are referred to as Event A and Event B, respectively.

The two white-light images shown in Figures 1(a) and 1(b) are recorded at 05:18 UT on 15 June and at the same time on 1 July, where the white circle represents the surface of the Sun and the one-quarter solid disk is where the LASCO C3 occulting disk is located. The size of each image is  $30 R_{\odot}$  along the horizontal direction and  $15 R_{\odot}$  along the vertical direction. The standard routines provided with the solarsoft software (<http://www.lmsal.com/solarsoft/>) are used to produce these images. A background representing the contribution of the F corona and instrumental stray light has been subtracted from each image. It can be seen that a well-defined streamer exists at the the southeastern part (PA= $119^{\circ}$ ) and the northeastern part (PA= $69^{\circ}$ ) in Figures 1(a) and 1(b), respectively. The blob structures that we are interested in are emitted right atop of these two streamers. To recognize the blobs clearly, in Figures 1(c) and 1(d) we present two running-difference images by subtracting the images taken one hour earlier from those shown in Figures 1(a) and 1(b). The blob structures are indicated with white arrows. In Figure 1(d), two blobs are emitted successively from the streamer. To view more blob events simultaneously in one figure, we produce the temporal evolutionary map, which is the stacked time series of radial strips centered along the corresponding streamer stalk in the running-difference images. This method has been used in previous blob studies (*e.g.*, Wang *et al.*, 1998; Wang *et al.*, 2000). The width of the narrow region is taken to be about 6 pixels, and the height is given by the C3 FOV. Such height-time maps are presented in Figures 1(e) and 1(f) for the two blob events, where the abscissa represents the time of observation and the ordinate the height of the strips.

It is obvious that the outward-moving blob structures are represented as white-black tracks in these height-time maps. By counting the number and deducing the slope of these tracks, we can easily obtain the daily rate and the velocity profiles of the blob structures. Note that only the data obtained by LASCO C3 are analyzed in this paper. The reason for excluding the C2 data is twofold. First, the blobs are observed initially near the streamer tips, which are generally located at about 2 to 4  $R_{\odot}$  in the middle part of the C2 FOV. At this height, it is generally difficult to discern the blob structures even from the running-difference images since the intensity of the background streamer emission is relatively strong. The seeing condition of blobs gets better when they enter the C3 FOV starting from 3.7  $R_{\odot}$ . Second, the C3 FOV already covers the outer part of the C2 FOV and our main purpose of this study is to search for the persistent and quasi-periodic release events of blobs and to determine the associated solar wind velocity, which is thought to be well fulfilled by only using the C3 data.

As can be seen from Figures 1(e) and 1(f) there are a total of 12 blobs observed during the three days from 13 to 15 June and 10 blobs from 30 June to 2 July with an average daily rate being 4 and 3.3, respectively. By fitting the apparent blob tracks with a second-order polynomial of the form  $r = r_0 + v_0t + \frac{1}{2}at^2$ , where  $r_0$  and  $v_0$  represent the heliocentric distance and speed at the starting point of the selected event, the constant acceleration  $a$  can be determined by the quadratic fit. The temporal derivative of this equation gives the expression of the fitted blob speed as  $v = v_0 + at$ .

The fitted velocity profiles as a function of heliocentric distance are plotted in Figures 1(g) and 1(h) for the two events discussed. Different symbols represent the velocities of different blobs; the numbers before the symbols are ordered according to the temporal sequence of the blob occurrence. As mentioned previously, the blob speed can be used as a proxy for that of the mean solar wind projected to the sky plane beyond a heliocentric distance of about 5-7  $R_\odot$ . We see that for most distances involved in Figures 1(g) and 1(h) the symbols can be regarded as velocities for both the blobs and the associated solar wind along the streamer stalks. The velocities increase gradually with increasing distances from 3.7 to 20  $R_\odot$ . Also, it can be seen that the velocities at a fixed distance vary significantly from blob to blob. To indicate this, in Table 1 we present the varying ranges of the blob velocities at 9  $R_\odot$  for all events. We see that, for Event A, the minimum and maximum of the blob (or the solar wind) velocities at 9  $R_\odot$  are 228 and 379  $\text{km s}^{-1}$ , respectively. The relative velocity variation is 66% for this event and 77% for Event B.

To reveal more details of the velocity variability, in Figure 2 we plot the fitted velocities at three heliocentric distances of 6  $R_\odot$  (squares), 9  $R_\odot$  (circles), and 12  $R_\odot$  (triangles) for Event A [Figure 2(a)] and B [Figure 2(b)]. The abscissa of this figure is the time starting from 0 UT of the first day of the event. It can be clearly seen that the speeds of different blobs at a fixed distance vary significantly with time. There are two possible physical causes accounting for such large temporal velocity variations at a fixed distance. The first one is the variation of the velocity of the local solar wind plasma, and the second one is the change of the projection angle caused by solar rotation during an event. We see that there is no apparent regular pattern governing the velocity variations at the three distances. Moreover, large velocity variations can take place within a few hours. For example, for the first two blobs shown in Figure 2(a) the velocity decreases abruptly from 430 to 280  $\text{km s}^{-1}$  at 12  $R_\odot$  and from 355 to 242  $\text{km s}^{-1}$  at 9  $R_\odot$ . The two blobs are separated temporally by several hours. In such a short time, the effect of solar rotation on the projection angle is basically negligible. Besides, if the temporal change at a certain distance was caused by the projection effect, the velocity would tend to be either monotonic or first increase then decrease. Therefore, we suggest that the velocity change presented in Figure 2 is mainly attributed to the velocity variability of the local solar wind plasma. It is well known that large velocity variability is one of the most apparent characteristics of the slow solar wind (*e.g.*, McComas *et al.*, 2000). It has also already been mentioned in the previous section that the wind along the plasma sheet above a streamer is usually regarded as one source of the slow solar wind; therefore, it is reasonable to deduce that this study provides an observational

manifestation of the large velocity variability of the slow solar wind near the Sun.

Using exactly the same method of data reduction as that for these two events, we examine the other eight events listed in Table 1. The PA of the streamer axis, the total number and the average daily rate of blobs in each event are shown in the third and fourth columns of Table 1. The obtained height-time maps showing the blob tracks are shown in Figure 3. The time of observation is taken to be the abscissa, and the height of the radial strips cropped from the series of running-difference images is shown as the ordinate of this figure, the same as in Figures 1(e) and 1(f). We can see that the most apparent common feature of the eight panels in Figure 3 is the persistent and quasi-periodic distribution of the white-black blob tracks. During each day of these events, we observe about three to five blobs released along the stalk of the corresponding streamer. The time span between two adjacent blobs is about five to eight hours. Note that a coronal mass ejection (CME) event was observed by LASCO C3 from 04:42 UT on 9 May, whose white-black track is obviously brighter than that of nearby blobs. For every blob release event, we have double-checked the white-light images of LASCO C3 to determine whether the white-black tracks in both Figure 3 and Figure 1 are caused by the small-scale blob events or the large-scale eruptive events. It is found that all the tracks are caused by small-scale blob events except the one mentioned here, which is not included in our statistics for the blobs.

In Figure 4, we plotted the velocity profiles of all the blobs shown in Figure 3. The velocities are obtained by the same method as that for Events A and B. Similarly to Figures 1(g) and 1(h), the velocities of different blobs are represented with different symbols, and the numbers in front of the symbols represent the temporal order of the blob occurrence. It can be seen that, in all these eight events, the blob velocities can vary significantly on a time scale of several hours to a few days. Again, there are no apparent patterns governing the velocity variations. For instance, from 14 to 16 February with 11 blobs detected, the velocities at a fixed distance, say,  $9 R_{\odot}$ , vary dramatically in a few hours from blob to blob. Specifically, the velocities of the first six blobs are 356, 229, 313, 326, 253, and 223  $\text{km s}^{-1}$ . As suggested previously, such large velocity variability should be taken as a consequence of the temporal evolution of the velocity of the local slow solar wind. In other words, the data analysis results shown in both Figure 1 and Figure 3 may provide observational evidence for the presence of large velocity variability of the slow wind near the Sun. Note that the varying ranges of the fitted blob velocities at  $9 R_{\odot}$  have been given in the fifth column of Table 1. In addition, the sixth column of this table presents the minimum and maximum values of the fitted acceleration, which also varies significantly from blob to blob. From the analysis, we suggest that the slow solar wind near the Sun flows outward from its source region already with both a highly variable speed and acceleration. It is apparent that both these two aspects may contribute to the large velocity variability of the slow wind observed *in situ* at much greater distances. We point out in passing that the PAs of the 10 streamers used in this study are distributed over a wide range from 67 to 288 degrees.

For all the blobs observed in the 10 events listed in Table 1, we plot the velocity versus height profile in Figure 5. It can be seen that the blobs generally accelerate gradually within the LASCO C3 FOV. Their velocities increase slowly from 50-150 km s<sup>-1</sup> at 3.7  $R_{\odot}$  and to 350-450 km s<sup>-1</sup> at 20  $R_{\odot}$ . These statistical results are in full agreement with previous results by Wang *et al.* (1998) using the data observed near the last solar minimum. We expect more persistent and quasi-periodic blob release events can be revealed in the future.

### 3. Summary and Discussion

In this paper we have examined the LASCO C3 data obtained in 2007 and found 10 persistent and quasi-periodic blob release events lasting for three to four days. The average daily rate of blobs is found to be three to five, in agreement with previous studies for the last solar minimum. It is found that the velocities of blobs vary significantly from blob to blob over a time scale of several hours to a few days. Taking the fitted blob speed beyond a certain distance as a proxy for that of the mean flow, we suggest that the large velocity variability, one of the most apparent signatures of the slow solar wind observed *in situ*, may develop near the Sun, say, within the first tens of solar radii.

Sheeley, Wang, and coauthors (Sheeley *et al.*, 1997; Wang *et al.*, 1998; Wang *et al.*, 2000) reported a few persistent blob release events around the last solar minimum. To interpret such steady blob releases from the tip of a streamer, Chen *et al.* (2009) proposed that the closed magnetic field geometry associated with a streamer cusp can become unstable to the expansion of the hot coronal plasmas, which results in a so-called intrinsic instability of corona streamers and the formation of blobs. For more details of this process, refer to the first section of this paper or to Chen *et al.* (2009). The modeled number density and velocity signatures, even the daily rate of blobs, are in agreement with previous observations. However, it is also apparent that not all streamers are associated with blobs. There are several possible reasons for this: *i*) The excitation and nonlinear development of the mentioned instability require certain specific physical conditions that develop over time. Blobs are not released, or, in other words, the instability does not develop or develop maturely, if the required conditions are not fulfilled or the developing process is disturbed by other coronal activities such as CMEs. *ii*) The brightness of the blob structures is only marginally higher than that of the background plasmas, so some blobs, even if released, are not observable owing to the limitations in resolution of current coronagraphs and interference from instrumental backgrounds (*e.g.*, stray light). *iii*) The blob signature may be obscured by other structures or eruptive phenomena in the foreground or the background corona along the line of sight.

The measurements of the dynamical parameters of the blob structures provide important complements to the other state-of-the-art techniques aimed at velocity diagnostics of the solar wind near the Sun. It may be expected that a distribution map of the solar wind velocities in the outer corona can be coarsely delineated with enough data accumulated. Although the flow velocity along the streamer stalk is provided only within a height ranging from a few solar radii to about



$20 R_{\odot}$ , it is still useful for constraining the solar wind condition in the outer corona. These constraints may help in establishing the background conditions that can be used in models for CME initiation and propagation, as well as for some space weather forecasting models.

From Figure 2, we see that velocities of successive blobs at a fixed distance can vary significantly within a few hours. Assuming streamer blobs to be velocity tracers of the slow solar wind along the plasma sheet, we therefore deduce that large velocity variability, observed *in situ* in the slow solar wind, is already manifested near the Sun. It is a good question to ask how the blob velocity variability compares with that of the slow solar wind. To address this question, we examined the solar wind velocity data obtained by, say, the *Ulysses*/SWOOPS instrument and found that large velocity variations similar to that presented in Figure 2 are not unusual. However, we point out that such comparisons should be conducted very carefully to reach a physically meaningful conclusion. This is mainly due to the large distance for the solar wind plasmas to travel from their source region to the point of *in situ* measurements. The original velocity profiles as revealed by the blob observations may undergo significant changes caused by the intrinsic dynamical evolution and coupling processes with nearby solar wind plasmas. The plasmas and magnetic structures associated with eruptive transient events, such as magnetic clouds, may also contribute to reshaping the solar wind velocity profiles. Therefore, comparison between the blob variability and the slow wind variability is in general not a trivial task, and so will not be further discussed here.

Another very interesting and meaningful study would be to search for the counterpart of the blob structures in interplanetary space with *in situ* data. As mentioned in the introduction, there are models that suggest the blobs originate from closed-field regions below the streamer cusp or along the current sheet in the open magnetic geometry; therefore, the determination of the *in situ* blob counterpart will be helpful to describe different formation mechanisms of blobs and to assess plasma properties in the region near the streamer cusp. Many spacecraft, such as *Ulysses*, SOHO, *Wind*, ACE, as well as the recently launched STEREO (Kaiser *et al.*, 2008; Galvin *et al.*, 2008), have already accumulated enough data that would be appropriate for this study. The *in situ* counterpart of a blob could be recognized by examining the elemental composition and abundance, ionic temperature, and charge-state distribution, as well as the magnetic-field geometry of the structures carried by the solar wind. This study should be conducted in future.

**Acknowledgements** The SOHO/LASCO data used here are produced by a consortium of the Naval Research Laboratory (USA), Max-Planck-Institut für Aeronomie (Germany), Laboratoire d’Astronomie (France), and the University of Birmingham (UK). SOHO is a project of international cooperation between ESA and NASA. This work was supported by grants NNSFC 40774094, 40825014, 40890162, and NSBRSF G2006CB806304 and by the Specialized Research Fund for State Key Laboratory of Space Weather in China. H.Q. Song is grateful to C.L. Shen, X.H. Zhao, and H.D. Chen for their assistance in preparing this paper.

## References

- Breen, A.R., Mikic, Z., Linker, J.A., Lazarus, A.J., Thompson, B.J., Biesecker, D.A., Moran, P.J., Varley, C.A., Williams, P.J.S., Lecinski, A.: 1999, *J. Geophys. Res.* **104**, 9847.
- Brueckner, G.E., Howard, R.A., Koomen, M.J., Korendyke, C.M., Michels, D.J., Moses, J.D., Socker, D.G., Dere, K.P., Lamy, P.L., Llebaria, A., *et al.*: 1995, *Solar Phys.* **162**, 357.
- Chen, Y., Li, X., Song, H.Q., Shi, Q.Q., Feng, S.W., Xia, L.D.: 2009, *Astrophys. J.* **691**, 1936.
- Cranmer, S.R., Kohl, J.L., Noci, G., Antonucci, E., Tondello, G., Huber, M.C.E., Strachan, L., Panasyuk, A.V., Gardner, L.D., Romoli, M., *et al.*: 1999, *Astrophys. J.* **511**, 481.
- Einaudi, G., Boncinelli, P., Dahlburg, R.B., Karpen, J.T.: 1999, *J. Geophys. Res.* **104**, 521.
- Endeve, E., Holzer, T.E., Leer, E.: 2004, *Astrophys. J.* **603**, 307.
- Endeve, E., Leer, E., Holzer, T.E.: 2003, *Astrophys. J.* **589**, 1040.
- Galvin, A.B., Kistler, L.M., Popecki, M.A., Farrugia, C.J., Simunac, K.D.C., Ellis, L., Möbius, E., Lee, M.A., Boehm, M., Carroll, J., *et al.*: 2008, *Space Sci. Rev.* **136**, 437.
- Grail, R.R., Coles, W.A., Klinglemith, M.T., Breen, A.R., Williams, P.J.S., Markkanen, J., Esser, R.: 1996, *Nature* **379**, 429.
- Habbal, S.R., Woo, R., Fineschi, S., O'Neal, R., Kohl, J., Noci, G., Korendyke, C.: 1997, *Astrophys. J.* **489**, L103.
- Kaiser, M.L., Kucera, T.A., Davila, J.M., Cyr, O.C.St., Guhathakurta, M., Christian, E.: 2008, *Space Sci. Rev.* **136**, 5.
- Lapenta, G., Knoll, D.A.: 2005, *Astrophys. J.* **624**, 1049.
- Lee, L.C., Wang, S., Wei, C.Q.: 1988, *J. Geophys. Res.* **93**, 7354.
- Li, X., Habbal, S.R., Kohl, J.L., Noci, G.: 1998, *Astrophys. J.* **501**, L133.
- McComas, D.J., Barraclough, B.L., Funsten, H.O., Gosling, J.T., Santiago-Muñoz, E., Skoug, R.M., Goldstein, B.E., Neugebauer, M., Riley, P., Balogh, A.: 2000, *J. Geophys. Res.* **105**, 10419.
- Sheeley, N.R., Wang, Y.M., Hawley, S.H., Brueckner, G.E., Dere, K.P., Howard, R.A., Koomen, M.J., Korendyke, C.M., Michels, D.J., Paswaters, S.E., *et al.*: 1997, *Astrophys. J.* **484**, 472.
- Strachan, L., Suleiman, R., Panasyuk, A.V., Biesecker, D.A., Kohl, J.L.: 2002, *Astrophys. J.* **571**, 1008.
- Suess, S.T., Wang, A.H., Wu, S.T.: 1996, *J. Geophys. Res.* **101**, 19957.
- Wang, S., Lee, L.C., Wei, C.Q.: 1988, *Phys. Fluids* **31**, 1544.
- Wang, Y.M., Sheeley, N.R., Socker, D.J., Howard, R.A., Rich, N.B.: 2000, *J. Geophys. Res.* **105**, 25133.
- Wang, Y.M., Sheeley, N.R., Walters, J.H., Brueckner, G.E., Howard, R.A., Michels, D.J., Lamy, P.L., Schwenn, R., Simnett, G.M.: 1998, *Astrophys. J.* **498**, L165.
- Woo, R., Martin, J.M.: 1997, *Geophys. Res. Lett.* **24**, 2535.
- Wu, S.T., Wang, A.H., Plunkett, S.P., Michels, D.J.: 2000, *Astrophys. J.* **545**, 1101.

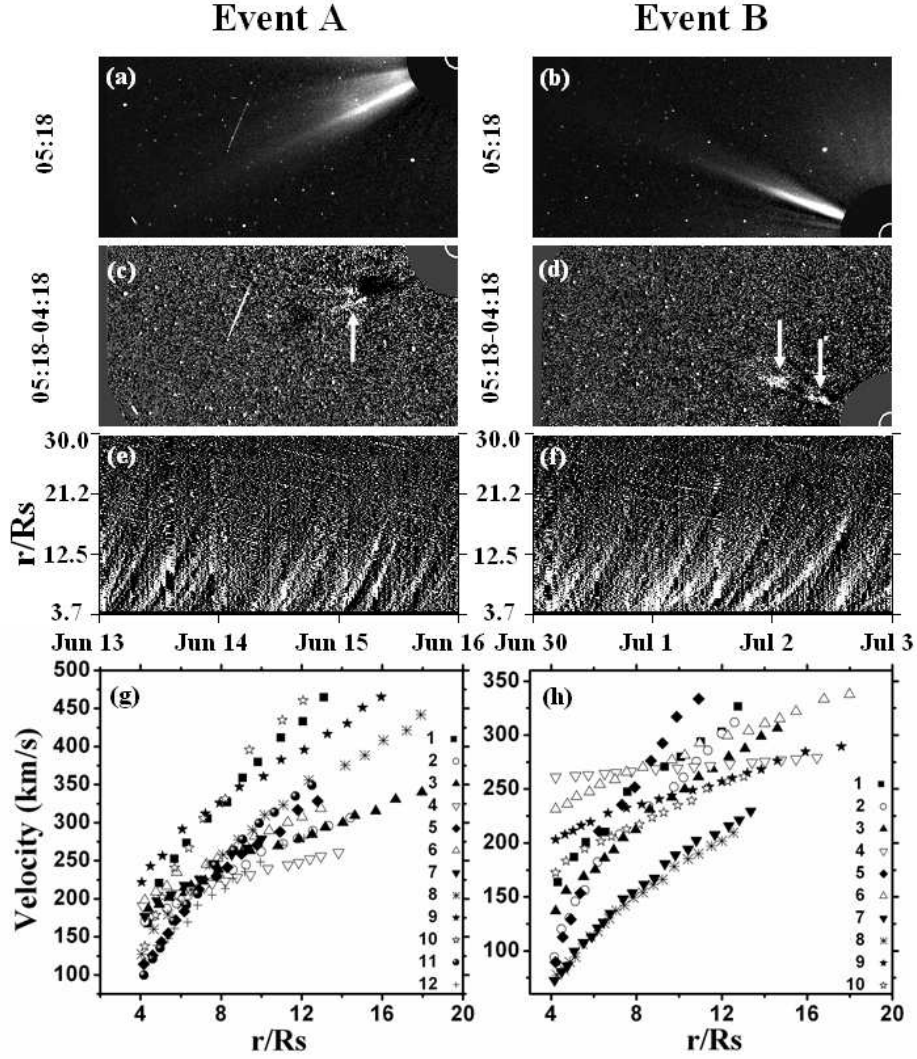


**Figure 1.** Two examples of quasi-periodic releases of blobs observed by LASCO C3, which are referred to as Event A (13-15 June) and Event B (30 June-2 July) in the text. In the eight panels, we show: instantaneous, background-subtracted images recorded at 0518 UT on 15 June (a) and 1 July (b) by C3, cropped to  $30 R_{\odot}$  in the horizontal direction and  $15 R_{\odot}$  in the vertical direction; the difference of images taken at 0518 and 0418 UT on 15 June (c) and 1 July (d) with the same size as that of panels a and b; height-time tracks of blobs for Events A (e) and B (f), which are produced by stacking radial strips centered along the streamer axis extracted from successive running-difference images; and the fitted blob velocities as a function of heliocentric distance (panels g and h for Events A and B). See text for more details.

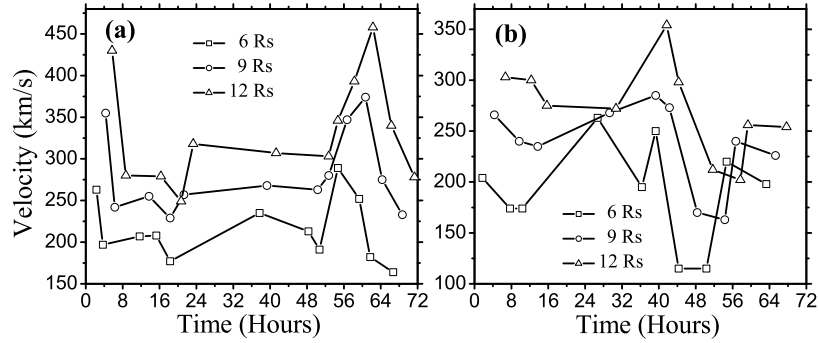


**Figure 2.** The fitted velocities at three heliocentric distances  $6 R_{\odot}$  (squares),  $9 R_{\odot}$  (circles) and  $12 R_{\odot}$  (triangles) for Events A (a) and B (b). The abscissa is the time starting from 0 UT of the first day of the event.

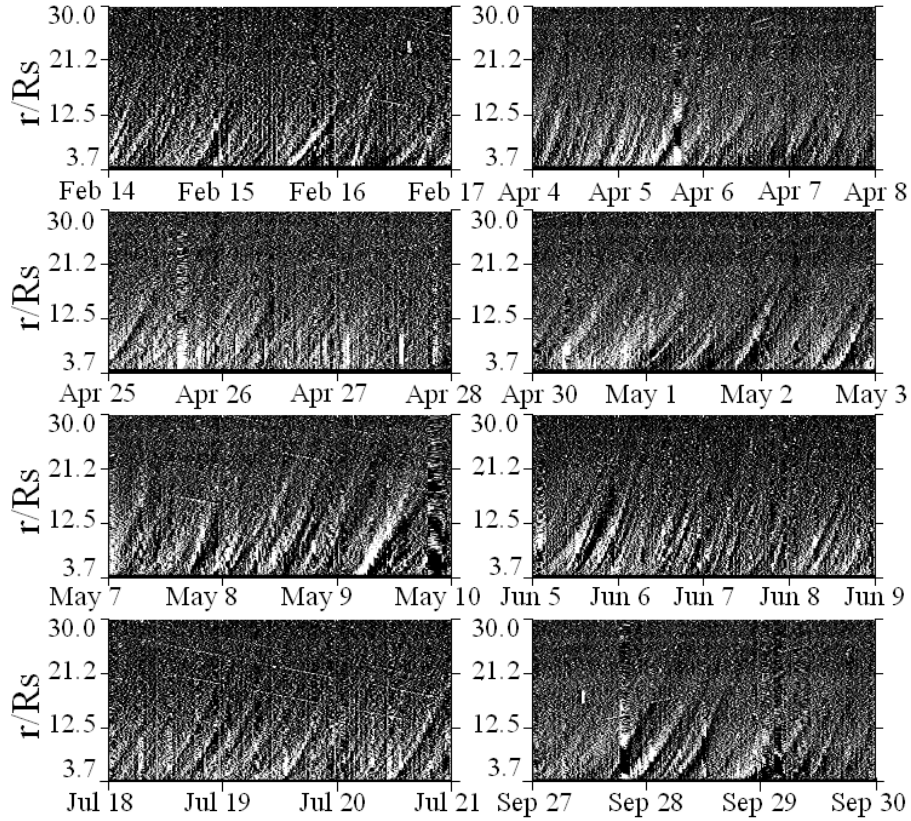


**Figure 3.** Height-time tracks of blobs for the eight events listed in Table 1. The images are produced by stacking radial strips centered along the streamer axis extracted from successive running-difference images of C3.

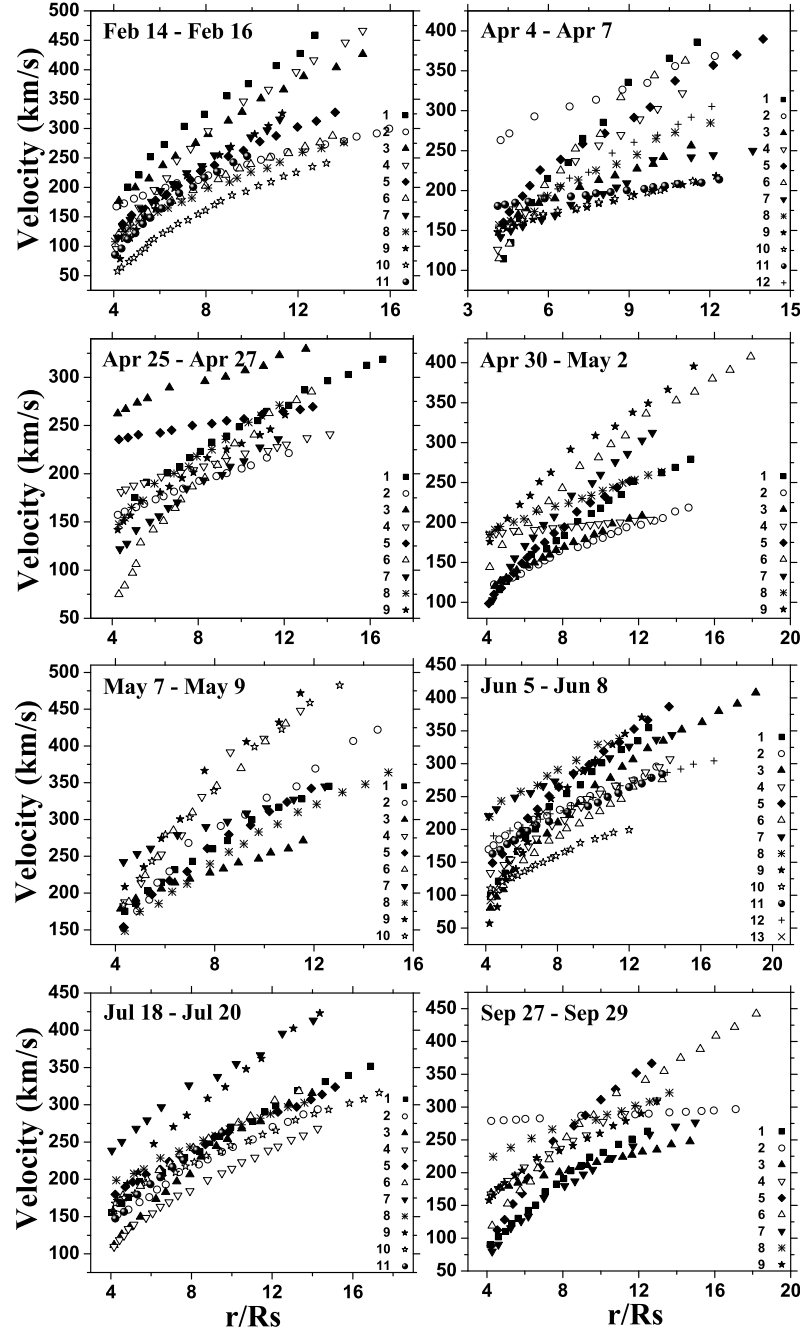
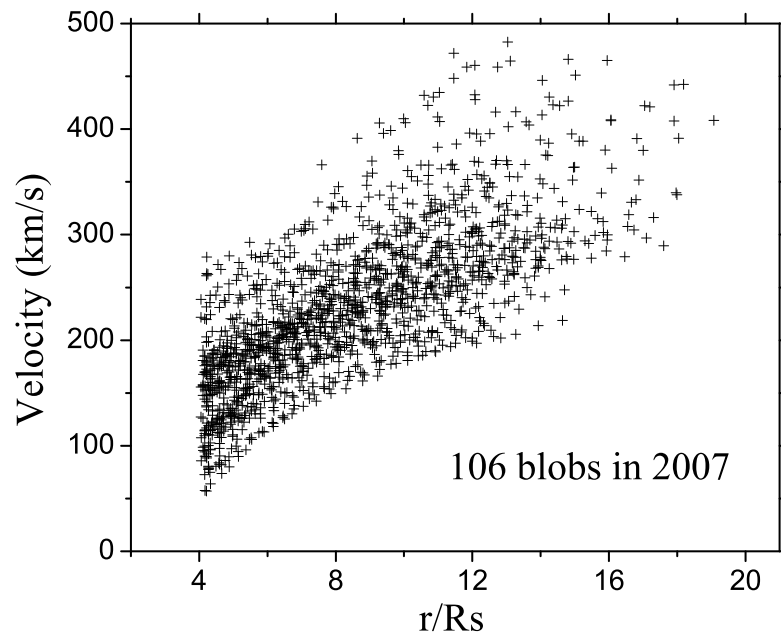


Figure 4. The fitted velocities of blobs as a function of heliocentric distance for the eight events listed in Table 1.



**Figure 5.** Scatterplot of velocity versus heliocentric distance for the 106 blobs observed in the 10 events listed in Table 1.